Available online at www.sciencedirect.com
SCIENCE DIRECT®
Global and Planetary Change 41 (2004) 81–93
GLOBAL AND PLANETARY CHANGE
www.elsevier.com/locate/gloplacha

Earth's orbital eccentricity and the rhythm of the Pleistocene ice ages: the concealed pacemaker

J.A. Rial*

Wave Propagation Laboratory, Department of Geological Sciences, University of North Carolina at Chapel Hill, NC 27599-3315, USA

Accepted 23 October 2003

Abstract

Most paleoclimate researchers would probably agree that variations in Earth's axial tilt and precession parameters have influenced past climate change. However, claims of connections between orbital eccentricity and ice age climate are more difficult to demonstrate or accept, especially since the amplitude of the strongest component of eccentricity-induced insolation, the 413-ky signal, is conspicuously small or absent from the power spectra of the last million years of paleoclimate data, and climate models without external forcing can easily reproduce the main ~100-ky cycles of the late Pleistocene and Holocene. Here I show that it is possible to tease out the 413-ky component of eccentricity directly from orbitally untuned deep-sea $\delta^{18}O$ time series, and that the signal is strong, albeit buried deep in the $\delta^{18}O$ time series, concealed by frequency modulation (FM). To extract the 413-ky signal, the data is frequency and phase demodulated numerically, while synthetic surrogate time series with properties believed similar to the actual data are used to test the nature of the modulator and the accuracy of each step in the inversion.

Keywords: Orbital eccentricity and the rhythm; Frequency modulation; Pacemaker

1. Introduction

After the discovery in 1976 (Hays et al., 1976) that frequencies in the spectra of deep-sea climate proxies ($\delta^{18}O$ time series) match periodic variations in insolation, the Milankovitch (1941) astronomical theory became a widely accepted model to explain the Earth's climate of the Pleistocene and the periodic advance and retreat of the continent-size ice sheets (Imbrie et al., 1993). In its original form, the theory holds that the climate of the great ice ages varied in proportion to changes in insolation caused by small fluctuations in the earth's orbital eccentricity, obliquity and precession (longitude of perihelion), which have predominant periods of ~100, 41 and 23 ky, respectively (1 ky = 1000 years; 1 ka = 1000 years ago). Although most indications are that variations in Earth's axial tilt and precession influence climate change, any connections between eccentricity and ice age climate periodicity are still poorly understood. This is in part because nonlinear climate models that require little if any astronomical input (Saltzman and Verbitsky, 1994), or nonlinear interactions of the precessional components (Ghil, 1994), can closely

* Tel.: +1-919-966-4553; fax: +1-919-966-4519.
E-mail address: jar@email.unc.edu (J.A. Rial).

0921-8181/$ - see front matter © 2004 Elsevier B.V. All rights reserved.
doi:10.1016/j.gloplacha.2003.10.003

reproduce the typical ~100-ky ice age cycles. In addition, lack of clear evidence for the presence of the strong 413-ky eccentricity component in the $\delta^{18}O$ time series of the last million years (Imbrie et al., 1993) has stimulated the search for astronomical forcings other than eccentricity (Muller and MacDonald, 1997) and for ice sheet dynamics capable of free oscillating at the right period without external forcing (Kallén et al., 1980). Informative surveys on the present status of Milankovitch's astronomical theory of the climate have been published recently (Hinnov, 2000; Elkibbi and Rial, 2001).

A sort of intermediate approach, by the author and collaborators (Rial, 1999; Rial and Anaclerio, 2000; Elkibbi and Rial, 2001), proposes that both astronomical forcing and nonlinear climate response play substantial roles, and introduces the idea that the climate system transforms the amplitude modulated insolation into frequency modulated fluctuations of global ice mass. Specifically, simplified models of the climate suggest that the amplitude modulation of "carrier" signals (e.g., the 23-ky precession, 41-ky tilt and 95-ky eccentricity) is transformed by the climate system into frequency modulation (Rial, 2004). This is analogous to the electronic process by which the frequency of a carrier signal is changed in proportion to the amplitude of a relatively lower frequency signal (the *message* or *intelligence*), as in FM radio and television broadcasting (Lathi, 1998; Hund, 1942). Many well-known properties of electronic FM signals are in fact fully consistent with features of the paleoclimate data (Rial, 1999) that have puzzled researchers for years, such as the varying duration of the ice age cycle, the presence of combination tones of orbital frequencies (Ghil, 1994; Pisias et al., 1990), and, perhaps the most telling, the apparent absence of spectral power at 413 ky (Imbrie et al., 1993).

If the FM model is correct, the inverse operation on the data, that is, frequency demodulation of the $\delta^{18}O$ records to extract the climatic modulator, could help our understanding of global climate change mechanics. Demodulation is in essence an inversion process, and although a relatively simple procedure in telecommunications (any modem, radio or TV receiver can do it), it is less than simple when the data are paleoclimate time series. This is because the precise nature of the modulator is not known, and there are unique technical issues (the effects of time scale uncertainty, noise and multiple carriers) that must be resolved to insure that the demodulation process is reliable, and reflects understandable physics. This paper describes how standard methods of electronic demodulation are used to guide the demodulation of selected paleoclimate time series to extract the fundamental frequency modulator of the climate, which appears to be, as suspected, the 413-ky component of eccentricity-induced insolation.

1.1. The timing problem

In performing spectral analyses of the paleoclimate data, one is always confronted with the dilemma of how accurate is the chronology of the records. This basic problem permeates any paleoclimate signal analysis approach. Since, in the analyses that follow, the signal sought is long-period, the result is likely insensitive to localized errors in timing, since timing errors are assumed to be randomly distributed and independent through time. The long records (1–2 My) used in the analyses are thus timed by using constant sedimentation rates. This seems to work well, as will soon be demonstrated, although not without a few problems. Chronologies based on orbital tuning cannot be used because orbital tuning subtly forces the astronomical signal into the data (Rial, 1999). These considerations considerably reduce the number of records available because only a few reliable chronologies exist with minimal astronomical influence and long enough time series. Examples of time scales nearly free from astronomical influence are GT4, a glacial physics-based chronology developed for the Vostok ice core records (Petit et al., 1999) and the 'constant sedimentation rate' scale developed by Raymo (1997) to time $\delta^{18}O$ deep-sea sediment records. The former provides a non-orbital time scale, but only for the last 400 ky, while the latter is based on carefully selected magnetic and biostratigraphic data and appears valid for the last few million years. For the purposes of demodulation, both time scales are found to be useful.

I used orbitally untuned deep-sea $\delta^{18}O$ time series from published ODP web sites, and selected those series whose terminations can visually be made to closely fit the corresponding ones on the Vostok temperature proxy. The depth scale of the selected

$\delta^{18}O$ series is transformed into a time scale by multiplying by that (constant) sedimentation rate which maximizes the visual fit of the record with the Vostok data. As this is accomplished, signal features between interglacials often do not correlate or do so poorly, but no attempt is made to remedy this situation, which is likely due to localized changes in sedimentation rate, which may produce timing errors as large as $\pm$ 10 ky in some places. The intention of course is to use the simplest time scale that is also as free from orbital tuning as possible, even if it means sacrificing details, or data sets. The estimated sedimentation rate obtained by comparison with the ice core is then assumed to hold for the entire length of the deep-sea $\delta^{18}O$ sediment record. Obviously, the assumption of single constant sedimentation rate is likely to be wrong at places within any sediment record, but inconsistencies in timing which occur in short, random segments of the record should average out and have only a minor influence in the results, as will be shown with the help of surrogate (synthetic) data.

The usable records are few, because the assumption of constant sedimentation rate is very restrictive, and in some cases obviously wrong. On the other hand, the selected time series are unique records, nearly free of orbital tuning or similar artifacts that might incorporate unwanted signals and should reflect global climatic events. In the following, I report results of three $\delta^{18}O$ records with durations of up to 2 million years, ODP sites 659, 846 and 849. To obtain a quantitative measure of the range of possible variations in the demodulation results, I use a simple data-augmentation scheme: from each single time series (Site 659, say), an ensemble of slightly compressed and stretched versions of it is constructed by slightly increasing or decreasing (by not more than $\pm$ 5%) the original sedimentation rate used to time the series. Each member of a given ensemble has thus a constant sedimentation rate that is a small perturbation on either side of that which best fits the Vostok data. Typically, each ensemble contains 10 to 15 members, as many as necessary to provide a probable range of data variance as a function of timing error. The difference in duration between the extreme (shortest and longest) members of any given ensemble is ~100 ky, or 1 ky per every 10 ky of record, which is a probably fair estimate of the maximum timing error (Raymo, 1997).

1.2. The demodulation method

A noiseless, periodic signal frequency-modulated by a message $m(t)$ can be represented by the equation (Lathi, 1998):

$$f(t) = A\cos\{\omega_c t + k_f \int_{-\infty}^{t} m(\zeta)\mathrm{d}(\zeta)\} = A\cos\{\theta(t)\} \quad (1)$$

This is a particular case of the general formula for an angle-modulated signal, which includes both frequency modulation (FM) and phase modulation (PM), depending on whether the modulator is the integral of the message (FM), as in Eq. (1), or the message itself (PM). In Eq. (1) ω_c is the angular frequency of the unmodulated carrier (for instance, the 95-ky eccentricity signal and/or the 41-ky tilt signal), k_f is a measure of the intensity of the modulation and A is a constant amplitude. The modulator (or message) $m(t)$ is in general an arbitrary function of time. The simplest FM signal, usually called single-tone modulation, occurs when $m(t)$ is a single sinusoid (Cuccia, 1952), while a strongly nonlinear 'multitone' or multifrequency modulation occurs when $m(t)$ contains two or more sinusoids or is itself a modulated sinusoid. The spectral analyses reported below show that the paleoclimate data are consistent with the latter type, which makes the demodulation or inversion process a delicate one, requiring careful checking of every step of the analyses with synthetic or surrogate data that simulate the actual time series.

Mathematically, extracting the message or 'intelligence' $m(t)$ from the frequency modulated signal $f(t)$ in Eq. (1) is apparently a simple operation. First, one constructs the analytic function $\varphi(t) = f(t) + iH\{f(t)\}$, where $H\{\cdot\}$ is the Hilbert transform and $i = \sqrt{-1}$. Then, multiplying both sides of the exponential representation of $\varphi(t)$ by $\exp[-i\omega_c t]$ gives the new function $\chi(t) = \exp[-i\omega_c t]\varphi(t) = A\exp[i\psi(t)]$; where $\psi(t) = k_f \int_{-\infty}^{t} m(\zeta)\mathrm{d}(\zeta)$. The phase of $\chi(t)$ thus becomes directly proportional to the integral of the message, and its time derivative gives the instantaneous frequency of $\chi(t)$, which is the sought $m(t)$. If A is not a constant but a slowly varying time function $A(t)$ whose

spectrum does not overlap that of the FM signal, Bedrosian's theorem (Vakman, 1998) shows that $A(t)$ can still be considered a constant to compute the Hilbert transform. The above operation can thus be performed analytically on surrogate data to compare with the results using the actual paleoclimate time series. Fig. 1a,b illustrates the method using synthetic frequency modulated signals.

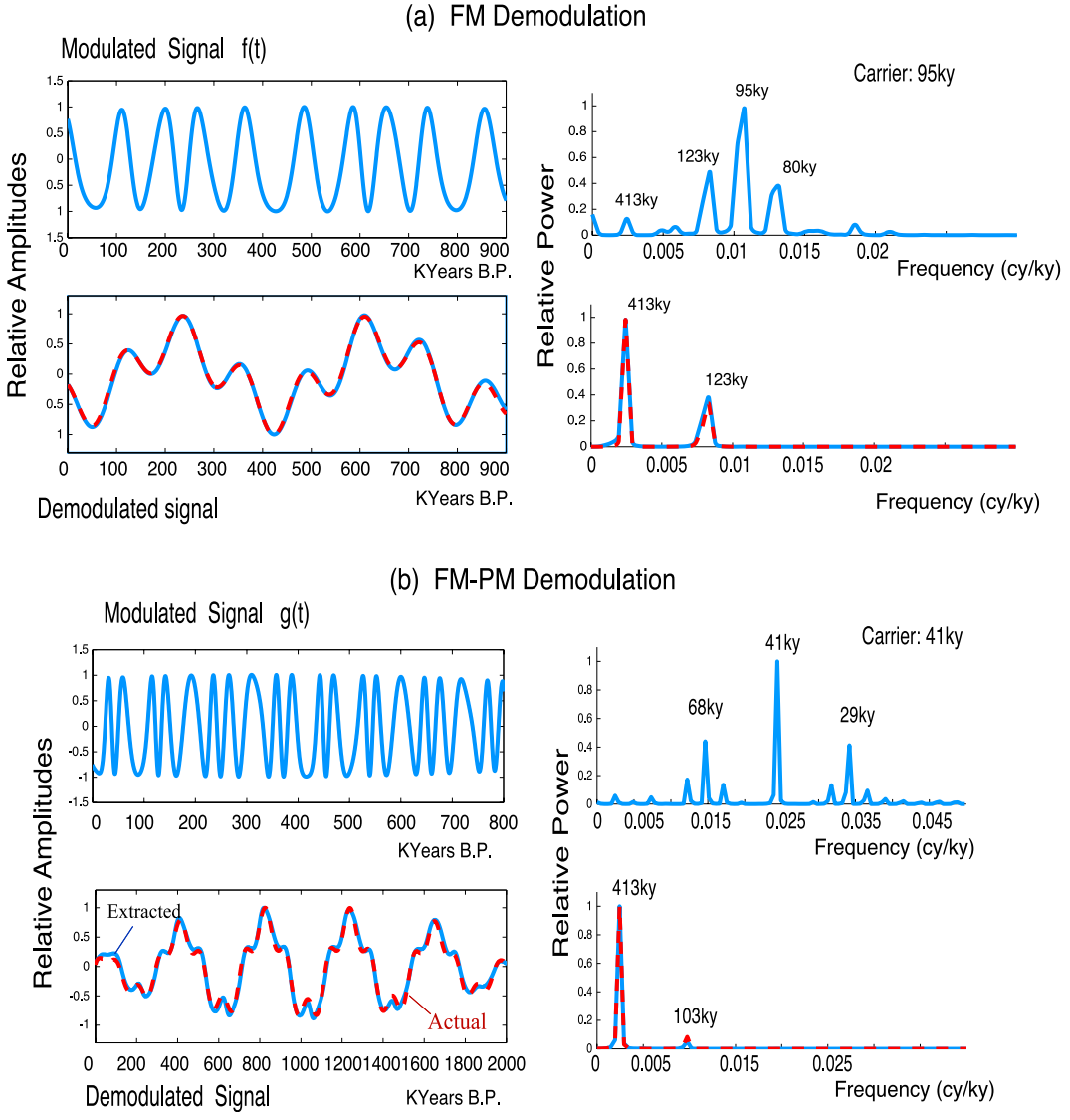

Fig. 1. (a) Illustration of the demodulation of a synthetic FM signal of the form $f(t)=\sin[2\pi t/95+k1\cos(2\pi t/413)+k2\sin(2\pi t/123)]$, where t is time in kiloyears and $k1$, $k2$ constants. The signal's spectrum is similar to that of paleoclimate data. Only one carrier is involved (the 95-ky signal). The numerically demodulated signal (modulator, continuous curve) is identical to that constructed (dashed), as shown in the time and frequency domains. (b) The demodulation algorithm is applied to a more complex signal with the form $g(t)=\sin\{2\pi t/41+a\sin[8\pi t/413+b\cos(2\pi t/413)+c\cos(8\pi t/413)]\}$, where the modulator itself is frequency modulated by two signals. As shown, the modulator is extracted without difficulty by the FM–PM demodulation (see text for details). Similarly, experiments have been performed with two carriers (the 95 ky and the 41 ky, say) with the spectral relative amplitudes obtained form the data. The algorithm performs correctly and extracts the sought modulator.

The foregoing formulation offers no difficulty, and the time-varying $\psi(t)$ can be easily extracted, unwrapped, detrended, tapered and differentiated to obtain $m(t)$.

However, since nothing is known in advance about the nature of $m(t)$ and random timing errors or interference from other carriers may distort the result of the inversion, every step of the process is accompanied by a comparison with results using surrogate data which are applied the exact same demodulation steps, as will be shown shortly. Experiments were carried out with two equally modulated carriers (95 and 41 ky) with the observed amplitude ratio, and the algorithm performed correctly, extracting the modulator accurately.

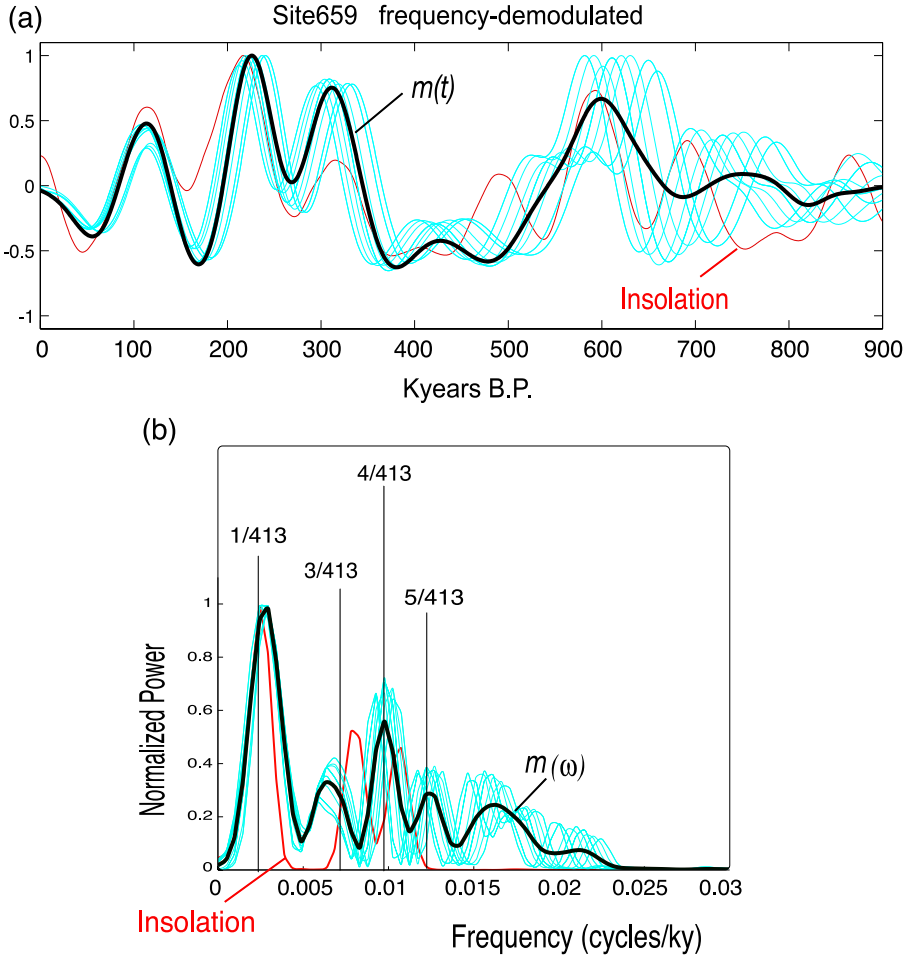

Fig. 2. (a) The result of frequency demodulating the time series from Site 659 is shown. The light lines are the demodulation results for all members of the data ensemble, that indicate the effect of ± 5% changes in sedimentation rate. The thick line is the average over the ensemble, the estimate of the presumed modulator $m(t)$. Note the similarity between $m(t)$ and the insolation curve. (b) The power spectra of the signals in (a) is dominated by a ~ 400-ky component. Before calculating the spectra, all signals are low-pass filtered with corner at 0.02 cy/ky. Note that the high frequency spectral peaks of $m(\omega)$, the power spectrum of $m(t)$, do not coincide with those of the insolation's. but rather with the higher harmonics of 1/413 ky^{-1}. It is apparent that $m(\omega)$ is composed of seemingly discrete, harmonically related frequencies, with spectral peaks located at regular intervals multiple of 1/413 ky^{-1}. These features suggest that $m(t)$, which is a modulating signal or modulator, is itself a frequency (or phase) modulated signal whose carrier is the harmonic 4/413 ky^{-1} (see text for details).

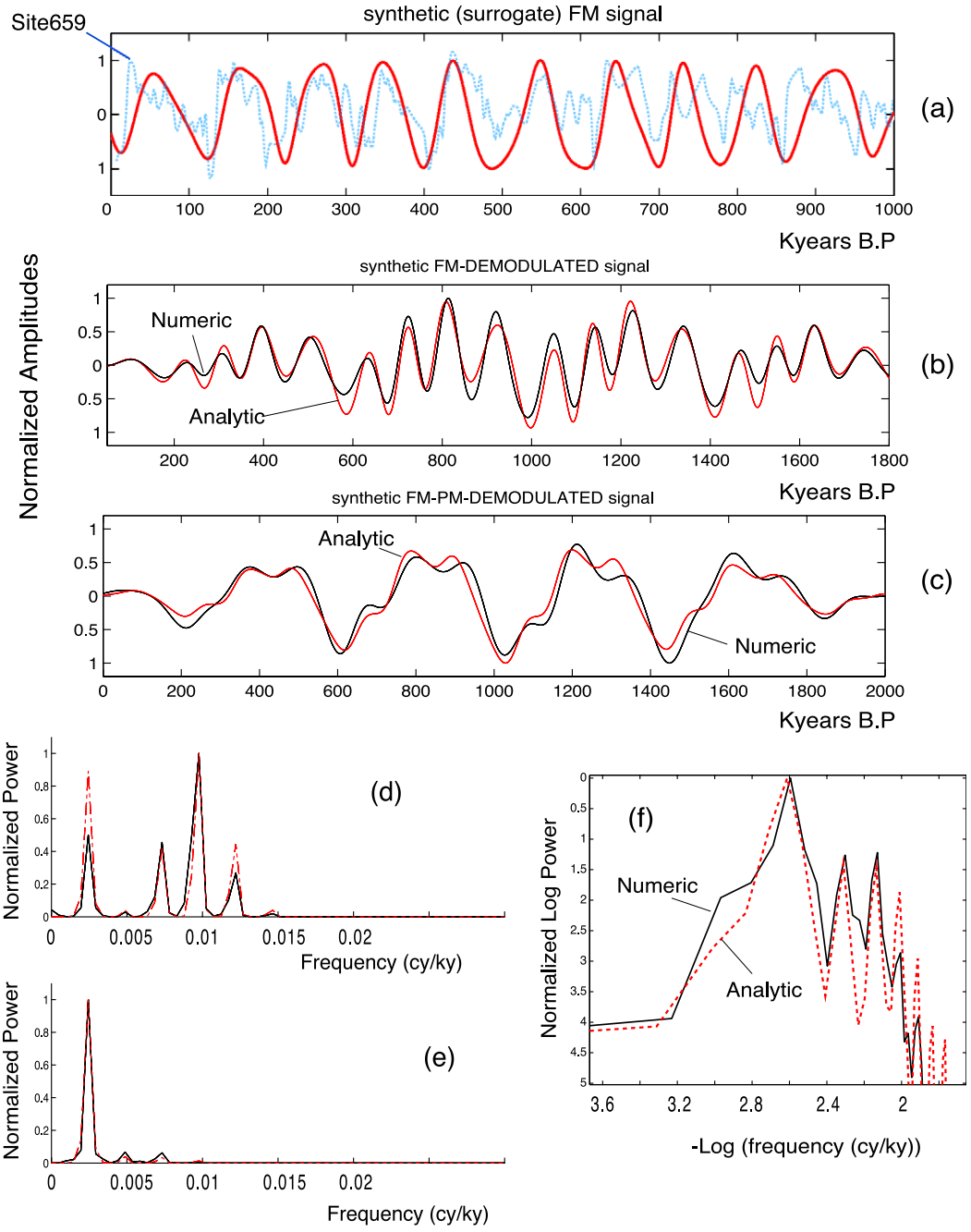

Fig. 3. The full demodulation process exemplified using surrogate signals. (a) A surrogate FM synthetic signal is compared to the actual data. The time-varying phase of the modulator is extracted by a two-step process: frequency demodulation (b), followed by phase demodulation (c). The two steps are required since the modulator $m(t)$ is itself a frequency (or phase) modulated signal. The time series (b) and the power spectrum (d) of the frequency demodulated surrogate signal are similar to the observed (cf. Fig. 2a,b) and consistent with a modulated $m(t)$. The power spectrum of the extracted modulator (e,f) shows that the 413-ky signal is dominating. The analytic approximations and the exact numerical results are compared throughout and shown to be satisfactorily close, the discrepancies due to the approximation of the Hilbert transform in the analytic procedure (see text for details).

2. The nature of the modulator

The result of frequency demodulating the ensemble of 14 time series constructed from ODP Site659 is shown in Fig. 2a, compared to the 15 °N insolation time series (Laskar et al., 1993). The extracted modulator $m(t)$ in the graph is the mean of the demodulated ensemble, and as can be seen, its time series is similar in phase, relative amplitude and frequency content to the insolation forcing (Fig. 2a, b) with one notable difference: the spectral resolution is high enough (1/1000 ky^{-1}) to verify that, with the exception of the 413-ky component, the higher frequency spectral peaks of the extracted $m(t)$ do not coincide with those of the eccentricity-induced insolation (1/123 and 1/95 ky^{-1}), but rather they appear to coincide with integer multiples (higher harmonics) of 1/413 ky^{-1}. In other words, the message $m(t)$ in Site 659 seems to consist of the 413-ky eccentricity forcing and its third, fourth and fifth harmonics. At the same time, since the carrier frequency is the 95-ky ($=2\pi/\omega_c$) component of eccentricity (the 41-ky tilt is also a carrier but interference of its side bands can be shown to be negligible in this part of the spectrum), the presence of the fifth harmonic (82.6 ky) in the modulator is unusual, as modulating frequencies are expected to be lower than their carrier (Lathi, 1998), especially if natural processes are involved, as is the case here. A reasonable guess is that the modulator is itself frequency modulated, because then the 82.6-ky peak would be just a side band of the 103.25-ky harmonic carrier (413/4 = 103.25). A simple mathematical model for the frequency modulator in Eq.

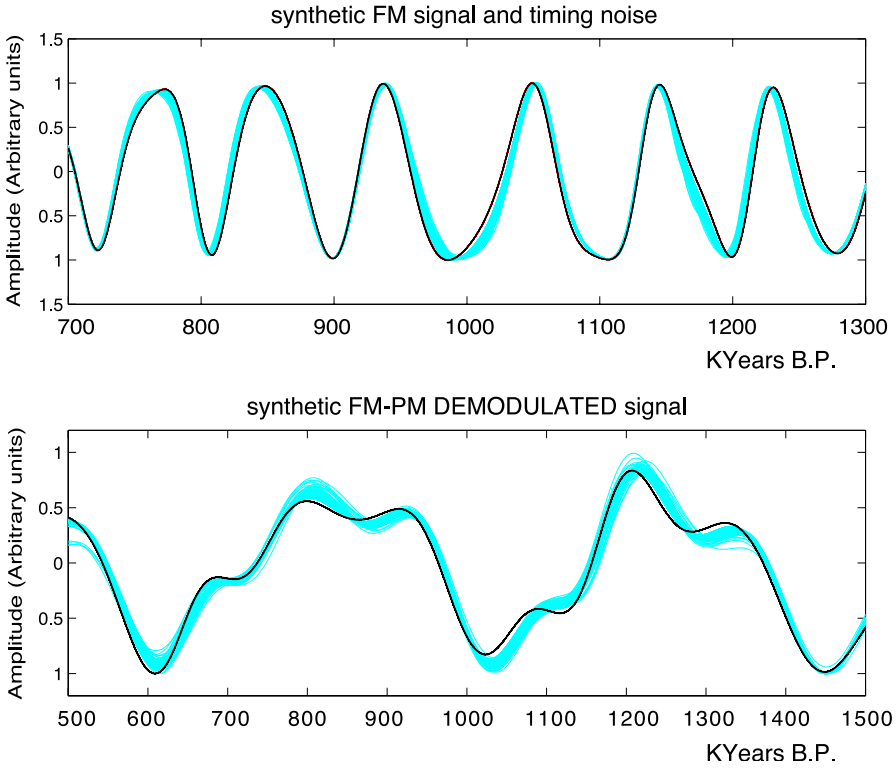

Fig. 4. The effect of random changes in the timing of the surrogate time series on the resulting inversion. The original signal is perturbed by randomly changing timing of the signal and constructing a new signal that has timing differences as large as ± 15 ky from the original. The effects on the extracted modulator are shown to be reasonable and only produce unimportant changes in the resulting spectrum. The timing errors are assumed random and normally distributed about the mean. For timing errors greater than 20 ky, deterioration of the extracted modulator is observed but the spectrum is still robustly showing most power at 413 ky (not shown).

(1) could thus have the form:

$$\int_{-\infty}^{t} m(\zeta)\mathrm{d}(\zeta) = k_0\sin(\omega_0 t) + k_1\sin[4\omega_0 t + k_2\cos(\omega_0 t)] \quad (2)$$

This is a sort of recursive modulation in which the 413-ky $= 2\pi/\omega_0$ component of insolation plays the fundamental role and whose spectral frequencies can be equated to the observed by appropriately tuning the adjustable parameters k_i. Since the 413-ky component has the most power in the eccentricity forcing (Laskar et al., 1993), it should not be surprising that it plays such an important role in the modulation. Since its fourth harmonic (103.25 ky $= 2\pi/4\omega_0$) acts as a modulated sub-carrier (Carlson, 1968), there is just one modulating signal or modulator, the eccentricity-induced 413-ky component of insolation, which is the message or intelligence sought for. Surrogate data computed using Eqs. (1) and (2) produce time signals and spectra very similar and consistent with those obtained when the frequency demodulation process is used on real data (Fig. 3).

The foregoing analysis strongly suggests that what has been defined as $m(t)$ in Eq. (1) is itself a phase-modulated function, so that its modulator (presumably the 413-ky cycle) has yet to be extracted. This is accomplished by constructing the analytic function $m(t)+iH\{m(t)\}$ and applying the formula:

$$\lambda(t) = \tan^{-1}\left[\frac{H\{m(t)\}}{m(t)}\right] \quad (3)$$

which is equivalent to phase demodulating $m(t)$.

It thus becomes apparent that the inversion requires two steps, frequency demodulation followed by phase demodulation, to recover the modulating signal, as illustrated in Fig. 3a–f. Tests using surrogate data are performed simultaneously with the inversion of the actual data to ensure that at least in principle the inversion scheme used is applicable to time series similar to the $\delta^{18}O$ records, that the algorithm is robust against reasonable errors in timing (see Fig. 4) and that interference from other carriers is minimal. If one can closely parallel the inversion of the paleoclimate time series with surrogate data, it is possible to conclude that for any original paleoclimate signal that is functionally similar to the model (Eqs. (1) and (2)), the numerical inversion successfully extracts the modulator.

Fig. 5 shows the final result of the two-step demodulation for Site 659. The inversion recovers a strong, single ~ 400-ky modulator in phase with the predicted 413-ky eccentricity component of insolation. This is quite an interesting result, because the 413-ky insolation forcing, believed too small or absent from paleoclimate time series (e.g., Imbrie et al., 1993), is made clearly visible as the only significant power in the demodulated signal.

It is important however to note that the duration of the Site 659 record is only slightly longer than two periods of the 413-ky modulator, so that the argument can be made that only with longer records (four or more periods long) can the presence of a 413-ky period harmonic be rigorously demonstrated, and a better spectral resolution obtained.

3. Extracting the modulator from longer (~2 My) records

To apply the foregoing analyses to longer records is difficult, because it requires that the single sedimentation rate assumption not be violated for a substantial length of core, and this makes the available data even scarcer than before. Fortunately, at least two suitably long records were found: ODP sites 849 and 846, with sedimentation rates calculated by Raymo (1997). These were successfully processed, as described in what follows.

Fig. 6a,b shows the results of demodulation of the Site 849 time series for the last 2 million years. The fit of the extracted modulator with the long-period insolation curve is remarkably good, except that the timing is off, mostly during the first 500 ky, which makes the extracted modulator appear acausal. This is interpreted as a change in sedimentation rate since in the time range 200–450 ky, it is observed that the Site 849 signal differs from other tuned records, such as Site 677. A simple change to a slower sedimentation rate between 200 and 450 ky produces a remarkably close fit with the phase of the insolation (Fig. 6b) and almost completely eliminates acausality. The period and relative amplitude of the corrected modulator also closely fit the long-term variations in insolation, which are controlled mainly by its 413- and ~ 800-ky components (Berger

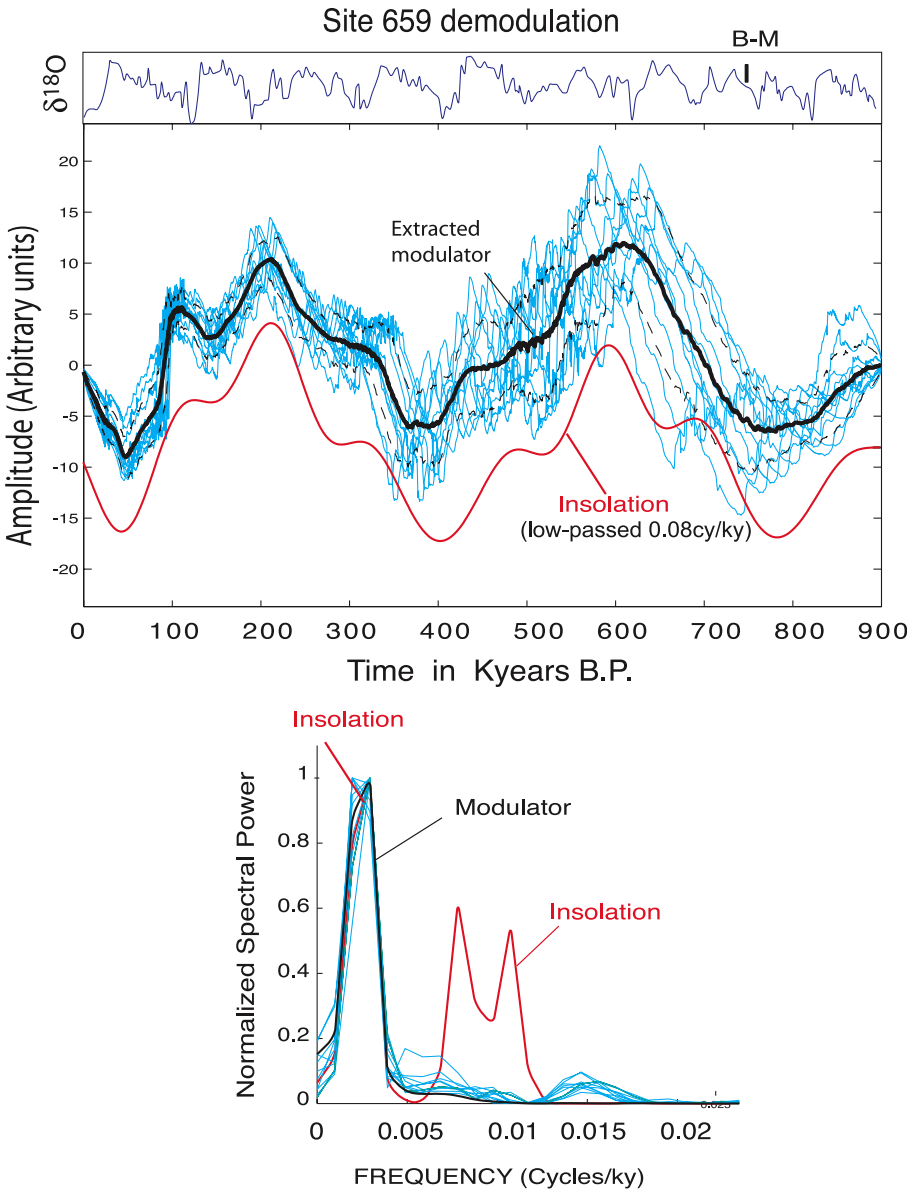

Fig. 5. The phase, period and relative amplitude of the extracted modulator closely fit the 413-ky eccentricity-driven insolation curve. The symbol B–M marks the Brunhes–Matuyama magnetic reversal on the $\delta^{18}O$ time series. (b) The power spectrum of the modulator is compared to that of the insolation. In the chosen time window (~ 900 ky long), most of the power of the modulator resides on the 413-ky component. Light lines in (a) and (b) are results for the ensemble and dashed lines mark one standard deviation from the mean.

and Loutre, 1991). That a 2-million-year-long record mimics the major features of the insolation curve so well suggests that the Earth's climate responds to and follows changes in orbital eccentricity, as the classic Milankovitch–Croll theory asserts. However, the climate system responds to this driving in a complex nonlinear way, transforming amplitude modulation into frequency modulation, and resonating with the astronomical forcing (Rial, 2004), in contrast to Milankovitch's vision of an essentially linear, unresponsive

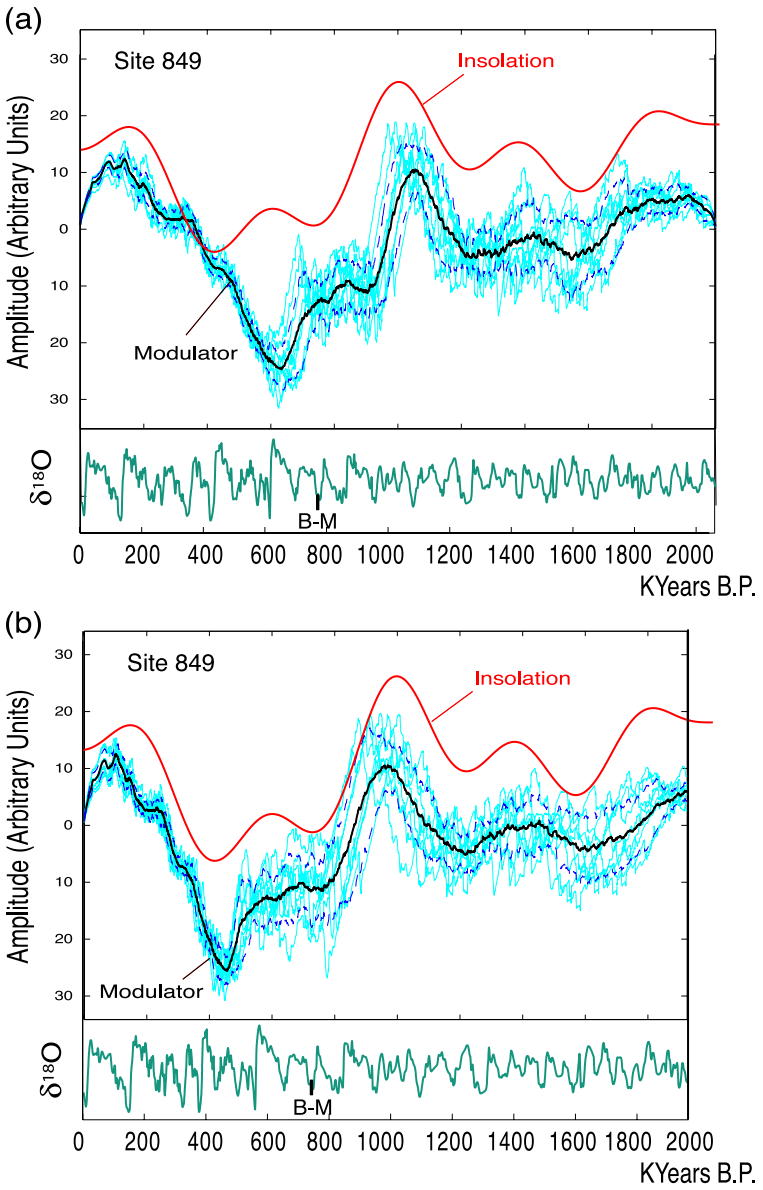

Fig. 6. As in Fig. 5, the modulator is extracted as the mean value of the ensemble constructed from the original Site 849 time series (see text for details). (a) shows the modulator of Site 849 compared to the long period (low-pass filtered) insolation curve over the last 2 million years. The similarity between the two curves is remarkable, although the extracted modulator timing is clearly off especially over the last 500 ky. However, assuming a 40% decrease in sedimentation rate from 200 to 450 ky BP makes the timing in this interval fit that of standard tuned records such as Site 677 and produces the close fit shown in (b). Note the timing change in the time series from (a). The result strongly suggests that the 413-ky eccentricity-driven insolation has driven the Pleistocene climate. Light lines are results for the ensemble and dashed lines mark one standard deviation from the mean.

climate system. Changes in sedimentation rate that violate the assumption of constant sedimentation rate may be responsible for the phase misfit (compare Fig. 6a,b), but even without a correction a single constant sedimentation rate clearly reveals the presence of the insolation signal (Fig. 6a). Fig. 7

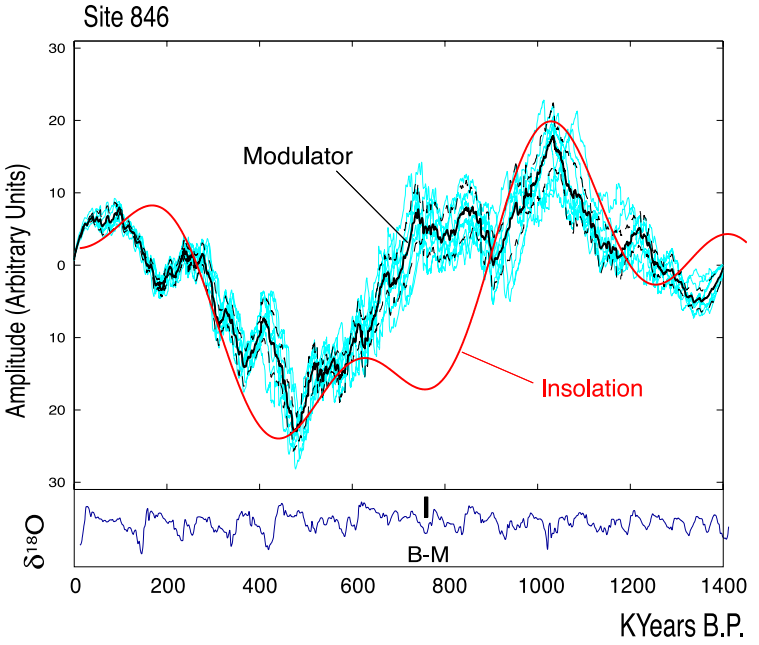

Fig. 7. As in Fig. 6 for Site 846. The extracted modulator is again consistent with the long-period insolation variation. The results in Figs. 6 and 7 provide a glimpse into the climate response at the time of the mid-Pleistocene transition (MPT), around 950 ka. This is the time around which a 41-ky-dominated glaciation cycle is transformed into a 100-ky-dominated one, as shown on the $\delta^{18}O$ records. The results indicate that at ~ 950 ka, the climate system response follows the rapid drop in insolation intensity starting at 1000 ka. Then starting at ~ 800 ka, the insolation levels out and remains lower than any time before for about 500 ky, a period that corresponds to the unprecedented growth of the ice sheets that profoundly changed the subsequent state of the global climate. It is tempting to conclude that nothing more extraordinary than a drop in the secular level of solar intensity is what caused the MPT. Light lines are results for the ensemble and dashed lines mark one standard deviation from the mean.

shows the result for Site 846 for the last 1.4 My. Again, only one sedimentation rate was used on each member of the ensemble. For the first 600 ky, the fit with the insolation curve is good and in general the shape of the modulator follows the insolation curve closely, except between 620 and ~ 900 ka where changes in the sedimentation rate are apparent.

4. Summary

Extracting the astronomical signal from the paleoclimate data has required two steps: frequency demodulation followed by the application of Eq. (3), which is essentially equivalent to phase demodulation. The paleoclimate data requires such treatment because it appears to be doubly modulated, with the modulating signal itself a modulated carrier. Coincidentally, *double frequency modulation*, or DFM, is a signal processing method commonly used in telecommunications (especially in satellite telemetry systems and wireless telephony) in which the sum of a number of modulated sub-carriers is used to frequency modulate a higher frequency carrier (Cartmell, 1990). This process efficiently handles multiple channels carrying very diverse types of information, so it is tempting to speculate that this is why it has been naturally selected for transferring astronomical signals into the climate system.

The modulators extracted from Sites 849 and 846 (which are both benthic records from the eastern equatorial Pacific basin but over 2200 km apart) show strong similarities as one should expect; and obvious differences, which are likely due to regional differences in sedimentation rate, also to be expected. The many similarities however are suggestive that the demodulation process is extracting the same signal (the 413-ky eccentricity and its sub-harmonic) form

both records, as it should. This is supported by the result of demodulating Site 659, which results in a signal dominated by the 413-ky eccentricity-induced component of insolation.

5. Why frequency modulation?

An important point remains to be dealt with and that is the reason or climate mechanism that causes frequency modulation. In a companion paper of this volume (Rial, 2004), I propose a system of differential equations that closely reproduces the observed FM effect in paleoclimate time series, including the Dansgaard/Oeschger (D/O) oscillations of the last glacial. In the model, the mechanism responsible for FM is the result of the climate system transforming the amplitude modulated astronomical forcing into frequency modulation. This is possible in a nonlinear climate system with variable thresholds, as shown in the simple mechanical analogue depicted in Fig. 8. Fig. 8a illustrates a simple system where a container with a siphon is continuously supplied with water at a constant rate (which simulates the growing of an ice sheet), causing the accumulation

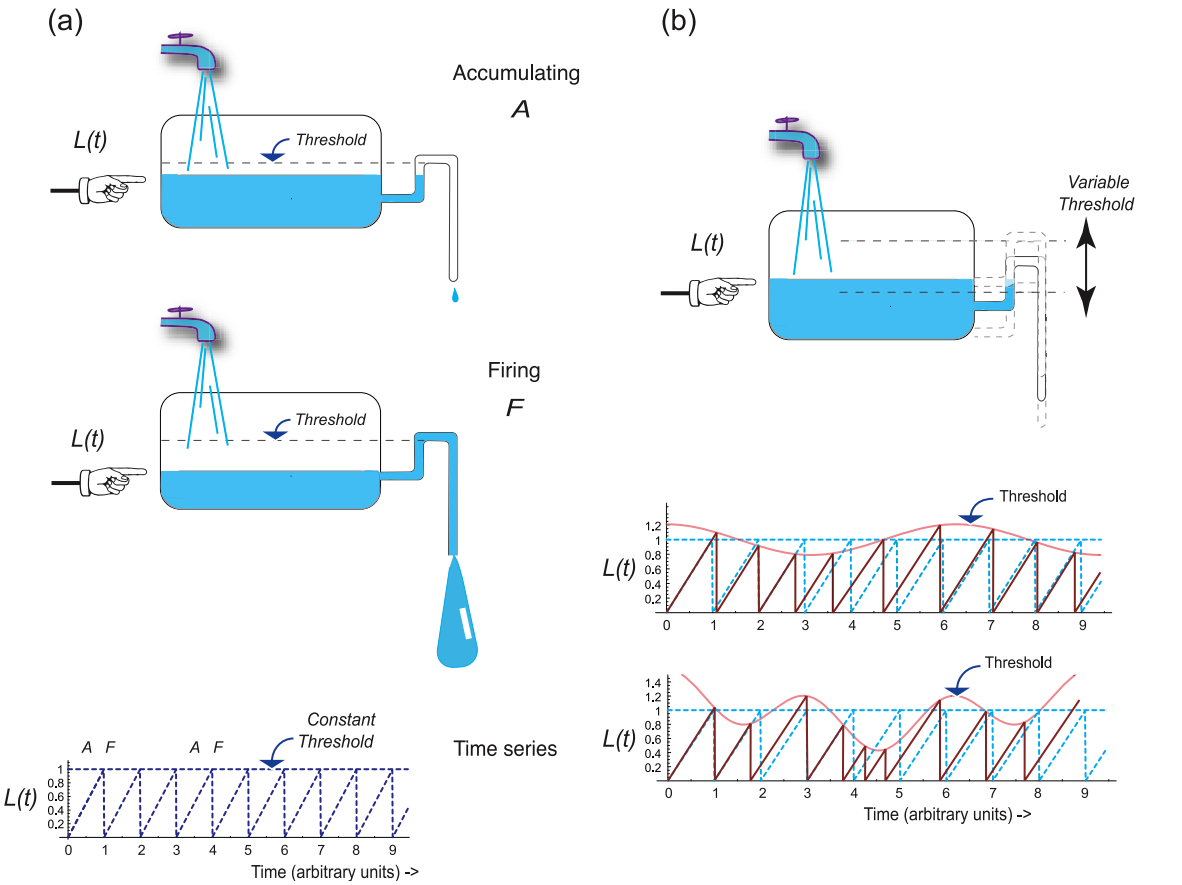

Fig. 8. (a) A mechanistic model of the climate system, represented by a 'leaky-bucket'. Water is supplied at a constant rate through the faucet. The siphon trap represents a threshold, held constant in (a). The water circulation mimics internal oscillations of the climate controlled by a constant threshold. The times series of the water level are analogous to the saw-tooth time series of climate records (see text for details). (b) When the threshold is made to vary due to external influences, the saw-toothed time series becomes frequency modulated, due to the imposed amplitude modulation of the height of the threshold (the trap). The climate analogy is described in terms of differential equations by Rial (2004). The FM effect can be subtle as in the middle diagram (simulates the deep-sea sediment FM effect), or drastic, as in the lower diagram (simulates the FM effect in the late glacial, such as the Dansgaard/Oeschger oscillations). See text for details.

A. The siphon's high level acts as a threshold, and so as soon as the water reaches it, the tank empties quickly (simulating an interglacial termination), down to the level of the container's outlet. In the actual climate, a threshold may be thought of as a point at which two competing feedbacks effects (positive feedback amplifies while negative feedback controls) are just balanced (Rial et al., 2004). For instance, in the absence of external perturbations, the threshold would represent the carrying capacity of the climate system (the maximum size the system allows the ice sheets to grow).

Once the lowest level of the water is reached the outpour ceases and the tank begins to fill again. The resulting time series is a saw-tooth with 'firings' happening at a constant time interval. This is the behavior of a (nonlinear) climate system evolving internally through the competing action of positive and negative feedbacks, and without 'external' influence (the water tap is assumed to be part of the system). Fig. 8b shows what happens when the threshold itself changes with time, driven by some periodic or quasi-periodic external forcing (such as the Milankovitch cycles). Frequency modulation clearly results and, depending on the strength of the forcing, the effect is subtle, as in the long period, deep-sea sediment records, or sharp and obvious, as in the D/O oscillations (see Rial, 2004).

Acknowledgements

This research was supported in part by grant ATM#0241274 from the National Science Foundation (Paleoclimate program). Comments from an anonymous reviewer, discussions with Lisa Sloan and Maya Elkibbi improved the manuscript.

References

Berger, A., Loutre, M.F., 1991. Insolation values for the climate of the last 10 million of years. Quaternary Science Reviews 10 (4), 297–317.

Carlson, A.B., 1968. Communication Systems: An Introduction to Signals and Noise in Electrical Communication. McGraw-Hill, New York.

Cartmell, M., 1990. Introduction to Linear, Parametric and Nonlinear Vibrations. Chapman & Hall, London.

Cuccia, C.L., 1952. Harmonics, Sidebands and Transients in Communication Engineering. McGraw-Hill, New York.

Elkibbi, M., Rial, J.A., 2001. An outsider's review of the astronomical theory of the climate: is the eccentricity-driven insolation the main driver of the ice ages? Earth-Science Reviews 56, 161–177.

Ghil, M., 1994. Cryothermodyamics: the chaotic dynamics of paleoclimate. Physica. D 77, 130–159.

Hays, J.D., Imbrie, J., Shackelton, N.J., 1976. Variations in the earth's orbit: pacemaker of the ice ages? Science 194, 1121–1132.

Hinnov, L.A., 2000. New perspectives on orbitally forced stratigraphy. Annual Review of Earth and Planetary Science 28, 419–475.

Hund, A., 1942. Frequency Modulation. McGraw-Hill, New York.

Imbrie, J., Berger, A., Boyle, E.A., Clemens, S.C., Duffy, A., Howard, W.R., Kukla, G., Kutzbach, J., Martinson, D.G., McIntyre, A.C., Mix, A.C., Molfino, B., Morley, J.J., Peterson, L.C., Pisias, W.L., Prell, W.L., Raymo, M.E., Shackleton, N.J., Toggweiler, J.R., 1993. On the structure and origin of major glaciation cycles: 2. The 100,000-year cycle. Paleoceanography 8 (6), 699–735.

Kallén, E., Crafoord, C., Ghil, M., 1980. Free oscillations in a climate model with ice-sheet dynamics. Journal of Atmospheric Dynamics 36, 2292–2303.

Laskar, J., Joutel, F., Boudin, F., 1993. Orbital, precessional and insolation quantities for the earth from −20 Myr to +10 Myr. Astronomy and Astrophysics 270, 533–552.

Lathi, B.P., 1998. Modern Digital and Analog Communication Systems. Oxford Univ. Press, New York.

Milankovitch, M., 1941. Canon of insolation and the ice-age problem. Royal Serbian Academy Special Publication, vol. 132, Konigliche Serbische Akademie, Belgrade (Translated from German, Israel Program for Scientific Translations; Jerusalem, 1969).

Muller, R.A., MacDonald, G.J., 1997. Simultaneous presence of orbital inclination and eccentricity in proxy climatic records from ODP Site 806. Geology 25, 3–6.

Petit, J.R., Jouzel, J., Raynaud, D., Barkov, N.I., et al., 1999. Climate and atmospheric history of the past 420,000 years from the Vostok ice core, Antarctica. Nature 399, 429–436.

Pisias, N.G., 1990. Nonlinear response in the global climate system: evidence from Benthic oxygen isotopic record in core RC13-110. Paleoceanography 5 (2), 147–160.

Raymo, M.E., 1997. The timing of major climate terminations. Paleoceanography 12, 577–585.

Rial, J.A., 1999. Pacemaking the ice ages by frequency modulation of earth's orbital eccentricity. Science 285, 564–568.

Rial, J.A., 2004. Abrupt climate change: chaos and order at orbital and millennial scales. Global and Planetary Change 41, 95–109 (this issue).

Rial, J.A., Anaclerio, C.A., 2000. Understanding nonlinear responses of the climate system to orbital forcing. Quaterly Science Review 19, 1709–1722.

Rial, J.A., Pielke, R., Beniston, M., Claussen, M., Canadell, J., Cox, P., Held, H., de Noblet, N., Prinn, R., Reynolds, J.F., Salas, J., 2004. Nonlinearities, feedbacks and critical thresholds within the earth's climate system. Climatic Change (in press).

Saltzman, B., Verbitzky, M., 1994. Late Pleistocene climate trajectory in the phase space of global ice, ocean state, and CO_2: observations and theory. Paleocenography 9 (6), 767–779.

Vakman, D., 1998. Signals, Oscillations and Waves Artech. House, Boston, Mass.